16th World Conference on Earthquake, 16WCEE 2017

Santiago Chile, January 9th to 13th 2017

Paper N° 4111

Registration Code: S-XXXXXXXX

OPTIMAL INTENSITY MEASURES FOR PROBABILISTIC SEISMIC ANALYSIS OF ABOVE-GROUND LIQUID STEEL STORAGE TANKS

H.N. Phan[(1)], F. Paolacci[(2)], P.H. Hoang[(3)]

[(1)] *PhD student, Roma Tre University, Italy, hoangnam.phan@uniroma3.it*
[(2)] *Assistant Professor, Roma Tre University, Italy, fabrizio.paolacci@uniroma3.it*
[(3)] *Associate Professor, The University of Da Nang - University of Science and Technology, Vietnam, hphoa@dut.udn.vn*

Abstract

Liquid storage tanks are vital lifeline structures and have been widely used in industries and nuclear power plants. In performance-based earthquake engineering, the assessment of probabilistic seismic risk of structural components at a site is significantly affected by the choice of ground motion intensity measures (IMs). However, at present there is no specific widely accepted procedure to evaluate the efficiency or sufficiency of IMs used in assessing the seismic performance of steel storage tanks. The study presented herein concerns the probabilistic seismic analysis of above-ground steel storage tanks subjected to several sets of ground motion records. The engineering demand parameter for the analysis is the compressive meridional stress in the tank wall, which could lead to an elephant's foot buckling failure mode at the bottom shell course of the wall. The efficiency and sufficiency of each alternative IM are quantified by results of time history analyses for the structural response and a proper regression analysis. According to the comparative study results, this paper proposes the optimal IMs with respect to the above demand parameter for a portfolio of steel storage tanks.

Keywords: steel storage tank; simplified model; intensity measure, nonlinear time-history analysis, probabilistic seismic demand model

1. Introduction

The evaluation of the seismic risk of industrial plants due to the damage of liquid storage tanks has been widely investigated in the past. In this respect, even though fragility curves are an essential ingredient of the risk assessment, they are often empirically rather than analytically evaluated [1]. However, in modern approaches like the performance-based earthquake engineering, the analytical evaluation is preferred. In fact, probabilistic seismic demand models based on numerical simulations are often used as an essential step for producing fragility curves. These probabilistic models are traditionally conditioned on an intensity measure (IM) and may be significantly affected by the representation of ground motion uncertainty. The most commonly used IMs are the peak ground acceleration (*PGA*) and the 5% damped elastic spectral acceleration at the fundamental period of the structure [$S_a(T_1)$]. *PGA* has widely been used to describe the horizontal ground motions owing to its natural relationship to inertial forces, while $S_a(T_1)$ is known as a perfectly efficient and sufficient IM for elastic single degree-of-freedom systems.

As mentioned in literature, an IM is defined as efficient if it yields a small variability of the structural response for a given value of IM. On the other hand, a sufficient IM is defined as the one that makes the structural response conditionally independent, given IM, of earthquake magnitude and source-to-site distance [2]. Shome et al. [3] represented a probabilistic seismic demand analysis for structures based on a coupling of probabilistic seismic hazard analysis and time history nonlinear analyses of the structural response. They have demonstrated that $S_a(T_1)$ is more efficient than *PGA*. However, recent studies have also demonstrated that $S_a(T_1)$ may not be particularly efficient nor sufficient for some structures (e.g., tall, long period buildings) or for near-source ground motions [4, 5].

The seismic response of tanks is different to the buildings because of the effect of the fluid-structure interaction. The initial forces in the liquid mass, which are produced by the seismic excitation of the tank base, generate hydrodynamic pressure distributions on the tank wall. This results in the over-turning moments and the shear forces at the tank base. The probabilistic seismic response of tanks has been widely studied in the past; nevertheless, at present there is no specific accepted procedure for the efficiency or sufficiency of IMs used in assessing the seismic performance of liquid steel storage tanks. A rare example of IM efficiency evaluation for tanks is reported by Buratti and Tavano [6], where the efficiency and sufficiency of IMs were investigated in terms of the maximum lateral displacement of the tank wall. The authors discovered that in this specific case, the peak ground displacement is the most efficient IM. Recently, Phan and Paolacci [7] performed a comparative study for the selection of IMs used in the assessment of the seismic vulnerability of anchored steel storage tanks. For a specific case of fix-based tank configurations, the authors suggested $S_a(T_1)$ as the most efficient IM for both slender and broad cases.

This study presented herein concerns the probabilistic seismic response analysis for both anchored and unanchored above-ground steel storage tanks. Four bins of ground motion records are selected in order to investigate the effects of the earthquake magnitude and the source-to-site distance on the selection of IMs. Six cases of anchored steel storage tanks, ranging from slender to broad configurations, are examined by using a probabilistic seismic response analysis. The main response of the tanks is selected as the compressive meridional stress in the tank wall. The efficiency of each investigated IM is quantified by computing the standard deviation from a proper regression model for the selected engineering demand parameter (EDP). The sufficiency is then analyzed by evaluating the correlation between the residuals of the above regression model and ground motion parameters. According to the comparative results, this paper suggests the optimal IMs with respect to the selected EDP for a given portfolio of steel storage tanks.

2. Intensity measures and probabilistic seismic demand model

Various well-known IMs are used in this study. The most commonly used IM is *PGA*. The peak ground velocity (*PGV*) and displacement (*PGD*) are also used as magnitude-dependent IMs. Another widely accepted IM is $S_a(T_1)$. This IM represents not only the characteristic of the ground motion but also the ground motion frequency content around the structural period. Other IMs include S^*, I_{NP}, Arias intensity (I_A), cumulative absolute velocity (*CAV*), and cumulative absolute displacement (*CAD*). The definition of each IM is summarized in Table 1.

Table 1. IMs used in this study

Intensity measure	Note
$PGA = \max\left\lvert \ddot{u}_g(t) \right\rvert$	Peak ground acceleration
$PGV = \max\left\lvert \dot{u}_g(t) \right\rvert$	Peak ground velocity
$PGD = \max\left\lvert u_g(t) \right\rvert$	Peak ground displacement
$S_a(T_1)$	Spectral acceleration at fundamental period
$S_a^* = S_a(T_1)\left(\frac{S_a(2T_1)}{S_a(T_1)}\right)^{0.5}$	[8]
$I_{NP} = S_a(T_1)\left(\frac{S_{aAV}(T_1 \ldots 2T_1)}{S_a(T_1)}\right)^{0.4}$	[9]
$I_A = \frac{\pi}{2g}\int_0^{t_f}\left[\ddot{u}_g(t)\right]^2 dt$	Arias intensity [10]
$CAV = \int_0^{t_f}\left\lvert \ddot{u}_g(t) \right\rvert dt$	Cumulative absolute velocity [11]
$CAV = \int_0^{t_f}\left\lvert \dot{u}_g(t) \right\rvert dt$	Cumulative absolute displacement

To evaluate the IM efficiency, a probabilistic seismic demand analysis based on the work of Cornell et al. [12] is presented. Assuming a lognormal distribution, the estimate of the median demand can be predicted by a power model, as expressed in Eq. (1).

$$D_m = aIM^b \tag{1}$$

This equation can be rearranged as Eq. (2) to perform a linear regression of the logarithms of the IM and response quantity,

$$\ln D_m = \ln a + b \ln IM \tag{2}$$

where D_m is the median estimate of the demand, a and b are the regression coefficients based on the collection of the peak demand and IM quantity (d_i–IM_i) from time-history analyses of the analyzed tank using a suite of n ground motions. The dispersion of the demand conditioned on the IM can also be estimated from the regression analysis of the seismic demand, as given in Eq. (3).

$$\beta_{d|IM} \cong \sqrt{\frac{\sum_{i=1}^{n}\left[\ln(d_i) - \ln\left(aIM_i^b\right)\right]^2}{n-2}} \tag{3}$$

The sufficiency of IMs is analyzed by evaluating the correlation between the residuals of the linear regression model (described in Eq. 1) with the aforementioned parameters involved in hazard calculation, e.g., the moment magnitude (M_W) and the source-to-site distance (R_{jb}). In particular, linear regressions are performed between the regression-residuals of d_i–IM_i and M_W or R_{jb} given in Eq. (4),

$$\ln\left(residual_{d_i-IM_i}\right) = c_0 + c_1 M_W \left(\text{or } R_{jb}\right) \quad (4)$$

where c_0 and c_1 are the linear regression coefficients.

3. Numerical model of examined tanks and input signal selection

In this paper, different configurations of liquid steel storage tanks, ranging from slender to broad ones, are selected as case studies for the parametric investigation (Table 2). The effect of the geometrical configurations, represented by the aspect ratio of the tanks, on the selection of IMs is investigated. The water level is filled up 90% of the tank height for all cases. The aspect ratios of the tanks range from 0.5 to 3. The mechanical properties of the tanks and the contained liquid are shown in Table 3.

The seismic response of ground supported atmospheric cylindrical tanks subjected to earthquakes has been widely studied in the past [e.g., 13-17]. The liquid mass can be ideally subdivided into two parts, an impulsive component, which account for the base motion and the deformability of the tank wall, and a convective component, whose oscillations cause superficial waves of different frequencies and a very low percentage of the mass and damping. While the impulsive mass (m_i) moves rigidly with the tank wall, the convective mass oscillates in different modes with mass (m_{ci}) whose importance decreases with the order of the mode i^{th}. As mentioned in literature, it is enough to consider only the first convective mode to reproduce correctly the sloshing effect of the liquid [e.g., 16, 17], especially for slender tanks. This approximation can be assumed sufficiently accurate also for broad tanks.

Table 2. Geometrical parameters of the case studies

Type	Name	H_t (m)	H (m)	R (m)	γ	t_{eq} (mm)	t_b (mm)
Anchored	Tank #1	15	13.5	4.5	3	6	8
	Tank #2	15	13.5	5.4	2.5	7	8
	Tank #3	15	13.5	6.8	2	9	8
	Tank #4	15	13.5	9.0	1.5	11	8
Unanchored	Tank #5	15	13.5	13.5	1	15	8
	Tank #6	15	13.5	27.0	0.5	28	8

Note: H_t is the height of tank, H is the height of liquid level, R is the radius of tank, γ is the aspect ratio of tank, t_{eq} is the equivalent thickness of tank wall, and t_b is the thickness of the base plate.

Table 3. Mechanical properties of the tanks

Component	Mechanical property	Value
Steel tank	Young's modulus	200,000 MPa
	Yield strength	235 MPa
	Density	7,850 kg/m^3
Water	Density	1,000 kg/m^3

The overturning effect of the liquid at the tank base can be reproduced by placing the masses m_i and m_c at heights h_i and h_c, respectively. A possible numerical model of the anchored tanks is represented in Fig. 1(a), where the impulsive and the convective motions are simulated by two viscoelastic oscillators with stiffness k_i and k_c and damping coefficients c_i and c_c, respectively. The damping ratios for convective and impulsive masses are taken as 0.5% and 2%, respectively, as suggested previously for steel liquid storage tanks [e.g., 16, 17].

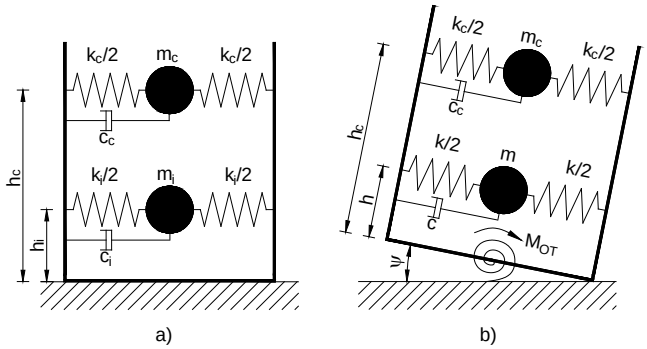

Fig. 1 – Simplified lumped mass model of the anchored (a) and unanchored (b) tanks

The partial uplifting of the bottom plate should be taken into account when tanks are subjected to strong seismic excitations. On this point, the uplifting mechanism of the unanchored broad tank is modeled by using the model proposed by [18, 19], where a rotational spring represented the rocking resistance of the base plate is added to the tank base, as shown in Fig. 1(b). In this model, the masses of the tank wall, m_w, and tank roof, m_r, are lumped with the impulsive mass. The total impulsive mass, $m = m_i+m_w+m_r$, is attached to the tank wall at an equivalent height, $h = (m_ih_i+m_wH_t/2+m_rH_t)/m$, by a viscoelastic oscillator with a stiffness, $k = \omega_i^2 m$, and a damping coefficient, $c = 2\xi_i m\omega_i$.

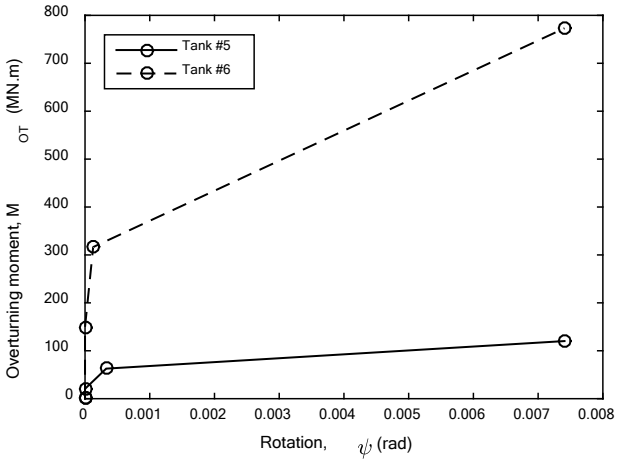

Fig. 2 – Relationships between overturning moment and base rotation of the broad tank

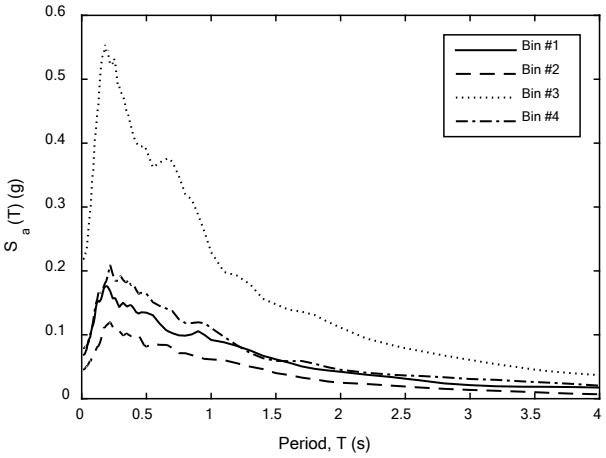

Fig. 3 – Median response spectrum for each bin of ground motion records

Table 4. Parameters of the tank models

Tank	m_i (T)	m_c (T)	T_i (s)	T_c (s)	h_i (m)	h_c (m)
#1	723	136	0.18	3.14	6.12	11.14
#2	1,002	235	0.17	3.44	6.10	10.72
#3	1,496	465	0.16	3.86	6.05	10.14
#4	2,357	1,079	0.16	4.44	5.93	9.32
#5	4,236	3,494	0.18	5.59	5.66	8.32
#6	9,275	21,643	0.22	9.04	5.40	7.33

The relationship between the base moment, M_{OT}, and the spring rotation, ψ, is established by the simplified method reported by Malhotra and Veletsos [20]. In this approach, the tank base plate is modeled using uniformly loaded, semi-infinite, prismatic beams that are connected at their ends to the cylindrical tank wall. The results of uplift force and uplift displacement can be obtained by solving the bending and string solutions. The M_{OT}-ψ relationship of the broad tank is shown in Fig. 3. The parameters of the simplified model for the examined tanks are shown in Table 4, where T_i and T_c are the natural periods of the convective and impulsive responses. The calculation of these natural periods is done in a similar manner as the one used in Eurocode 8 [21].

The ground motion records used as input for the numerical simulations are selected from PEER ground motion database. The records with moment magnitudes smaller than 5.5 and source-to-site distances greater than 100 km are excluded. The soil of the record stations is characterized by stiff soil conditions (360 m/s $\leq V_{s,30} \leq$ 800 m/s), which are in compliance with the Eurocode 8 [20] soil type B. In addition, two magnitude groups are presented including small amplitude ($5.5 \leq M_W \leq 6.5$) and large amplitude ($6.5 < M_W \leq 7.5$). Records are also classified into short distance ($0 \leq R_{jb} \leq 30$) and long-distance ($30 < R_{jb} \leq 100$). The selected 120 records are equally subdivided into four bins, as shown in Table 5, where $V_{s,30}$ is the average shear wave velocity. The median response spectrum of each bin are plotted in Fig. 3.

Table 5. Selections of ground motion records for four bins

Name	M_W	R_{jb} (km)	$V_{s,30}$ (m/s)	N° records
Bin #1	5.5 6.5	0-30	360-800	30
Bin #2	5.5-6.5	30-100	360-800	30
Bin #3	6.5-7.5	0-30	360-800	30
Bin #4	6.5-7.5	30-100	360-800	30

4. Comparative results

4.1 IM efficiency

Results of the comparative analysis on the efficiency of IMs are presented with respect to the four bins of ground motion records in Table 5. The IM efficiency is evaluated by computing the standard deviation ($\beta_{d|IM}$) and the coefficient of determination (R^2); the lower standard deviation (or the higher coefficient of determination), the higher IM efficiency.

The seismic response of the tanks presented herein is the compressive meridional stress in the tank wall (σ_z), which could lead to a major failure mode, i.e., the elephant's foot buckling at the bottom shell course of the wall. Due to a large difference of the natural periods of the impulsive and convective components of steel storage tanks, these two motions can be consider uncoupled. The seismic response of tanks is mainly affected by the impulsive component of the liquid motion. The fundamental mode of steel cylindrical tanks subjected to an earthquake excitation is associated with the first fundamental mode of a cantilever beam [13-17]. In this respect, the natural impulsive period of the tank models are used as the fundamental periods for calculating the frequency-dependent IMs. The comparative results in terms of $\beta_{d|IM}$ and R^2 for each IM regarding to the meridional stress response are shown in Tables 6-9.

The information reported in the tables shows that IMs exhibiting the highest efficiency are in the structure-specific group (frequency-dependent IMs), where includes information of the fundamental structure period. Among this group, the spectral acceleration at the fundamental period $S_a(T_1)$ is the most efficient IM in most of the cases. The use of I_{NP} also leads to a low dispersion as well, especially in the cases of unanchored tanks. In addition, the performance of S^* is lower than that of $S_a(T_1)$ and I_{NP} except the case of Tank #5 subjected to Bin #3 records.

Table 6. Bin #1, small amplitude, short distance

Tank	**#1**		**#2**		**#3**		**#4**		**#5**		**#6**	
	$\beta_{d\|IM}$	R_2	$\beta_{d\|IM}$	R_2	$\beta_{d\|IM}$	R_2	$\beta_{d\|IM}$	R_2	$\beta_{d\|IM}$	R_2	$\beta_{d\|IM}$	R_2
PGA	0.34	0.76	0.34	0.77	0.34	0.71	0.31	0.74	0.64	0.68	0.54	0.70
PGV	0.48	0.50	0.51	0.46	0.51	0.35	0.48	0.39	0.88	0.4	0.76	0.42
PGD	0.60	0.23	0.63	0.21	0.59	0.12	0.57	0.14	1.02	0.19	0.89	0.20
$S_a(T_1)$	**0.12**	**0.97**	**0.10**	**0.98**	**0.13**	**0.96**	**0.11**	**0.97**	0.5	0.81	**0.43**	**0.81**
*S**	0.22	0.90	0.25	0.87	0.28	0.80	0.25	0.83	0.53	0.78	0.57	0.67
I_{NP}	0.15	0.95	0.14	0.96	0.18	0.92	0.16	0.94	**0.46**	**0.84**	0.48	0.76
I_A	0.38	0.68	0.41	0.67	0.41	0.57	0.38	0.61	0.69	0.63	0.61	0.63
CAV	0.42	0.61	0.45	0.59	0.45	0.49	0.42	0.52	0.76	0.55	0.68	0.54
CAD	0.52	0.41	0.55	0.38	0.54	0.27	0.51	0.30	0.94	0.31	0.83	0.32

Table 7. Bin #2, small amplitude, long distance

Tank	**#1**		**#2**		**#3**		**#4**		**#5**		**#6**	
	$\beta_{d\|IM}$	R_2	$\beta_{d\|IM}$	R_2	$\beta_{d\|IM}$	R_2	$\beta_{d\|IM}$	R_2	$\beta_{d\|IM}$	R_2	$\beta_{d\|IM}$	R_2
PGA	0.23	0.80	0.25	0.75	0.30	0.56	0.28	0.62	0.53	0.74	0.32	0.68
PGV	0.47	0.17	0.46	0.15	0.43	0.10	0.43	0.12	0.98	0.11	0.51	0.19
PGD	0.50	0.07	0.48	0.06	0.44	0.04	0.45	0.05	1.02	0.03	0.54	0.11
$S_a(T_1)$	**0.12**	**0.94**	**0.11**	**0.95**	**0.10**	**0.95**	**0.10**	**0.95**	**0.36**	**0.88**	**0.18**	**0.90**
*S**	0.29	0.69	0.27	0.70	0.25	0.71	0.24	0.73	0.64	0.62	0.33	0.66
I_{NP}	0.17	0.89	0.15	0.91	0.15	0.89	0.14	0.90	0.40	0.85	0.22	0.85
I_A	0.34	0.57	0.34	0.52	0.34	0.44	0.33	0.47	0.76	0.47	0.39	0.54
CAV	0.38	0.46	0.38	0.42	0.36	0.36	0.36	0.39	0.83	0.36	0.43	0.43
CAD	0.50	0.08	0.47	0.08	0.44	0.07	0.44	0.07	1.02	0.04	0.54	0.11

Table 8. Bin #3, large amplitude, short distance

Tank	**#1**		**#2**		**#3**		**#4**		**#5**		**#6**	
	$\beta_{d\|IM}$	R_2	$\beta_{d\|IM}$	R_2	$\beta_{d\|IM}$	R_2	$\beta_{d\|IM}$	R_2	$\beta_{d\|IM}$	R_2	$\beta_{d\|IM}$	R_2
PGA	0.37	0.81	0.41	0.78	0.35	0.80	0.36	0.79	0.5	0.7	0.7	0.69
PGV	0.69	0.35	0.70	0.35	0.67	0.29	0.65	0.30	0.77	0.3	1.11	0.24
PGD	0.85	0.01	0.87	0.01	0.80	0.01	0.78	0.01	0.91	0.01	1.27	0.01
$S_a(T_1)$	**0.14**	**0.97**	**0.14**	**0.97**	**0.12**	**0.98**	**0.13**	**0.97**	0.49	0.71	**0.45**	**0.88**
*S**	0.29	0.88	0.28	0.90	0.26	0.89	0.26	0.89	**0.41**	**0.8**	0.64	0.75
I_{NP}	0.18	0.95	0.17	0.96	0.15	0.97	0.16	0.96	0.46	0.75	0.47	0.86
I_A	0.36	0.82	0.39	0.80	0.38	0.77	0.37	0.78	0.47	0.73	0.62	0.76
CAV	0.43	0.74	0.47	0.71	0.46	0.67	0.44	0.68	0.54	0.66	0.68	0.71
CAD	0.78	0.15	0.81	0.14	0.76	0.09	0.74	0.10	0.86	0.12	1.20	0.10

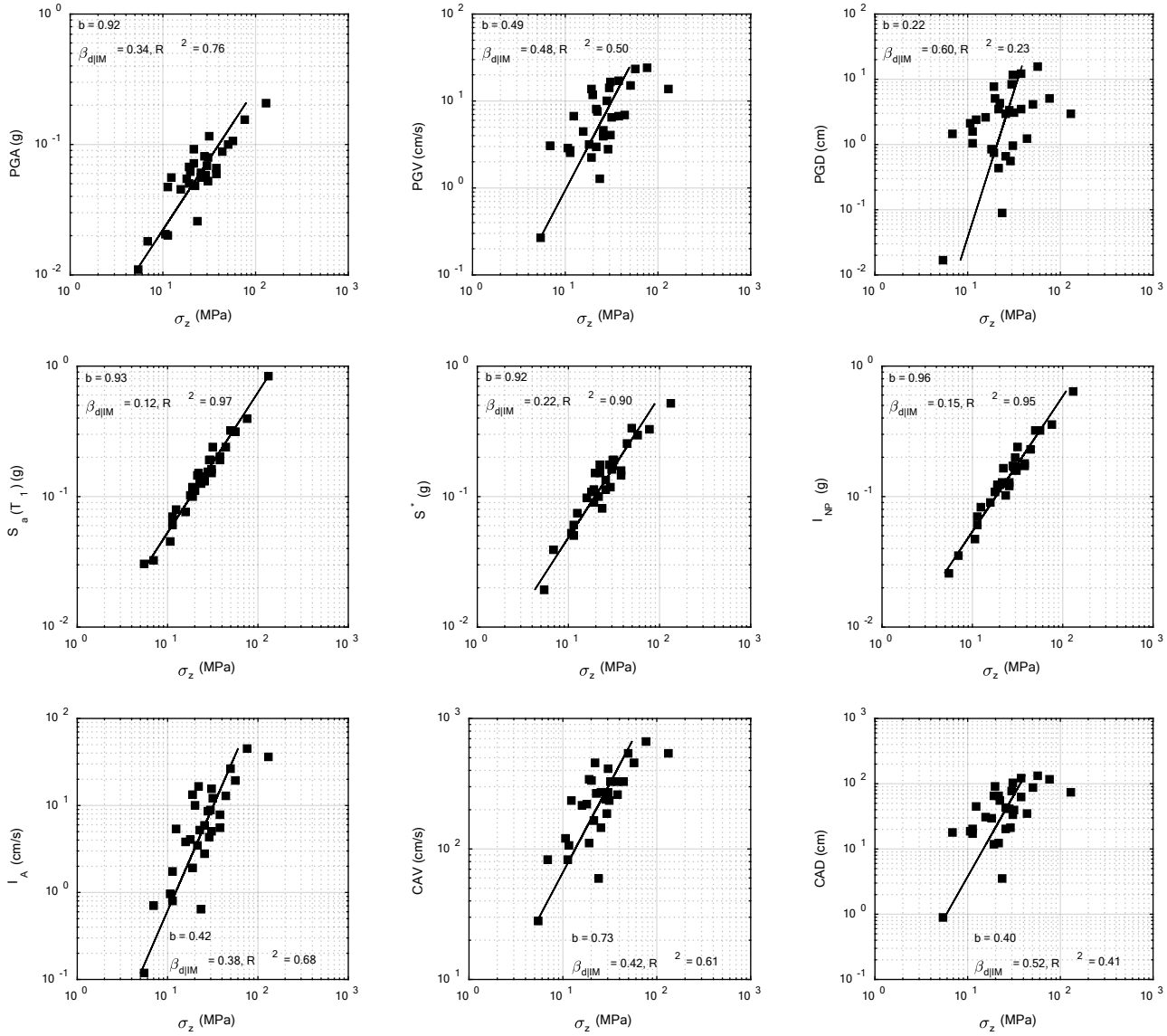

Fig. 4 – Linear regression analysis results for Tank #1 subjected to Bin #1 records

Among magnitude-dependent IMs, *PGA* shows the best performance for all the cases. In contrast, *PGD* shows the weakest performance, especially in the cases of large amplitude records. The results also show that the efficiency of this IM group is typically lower than that of the frequency-dependent IMs.

In the case of duration-dependent IMs, I_A appears as the most efficient one. *CAV* produces instead a slight increase of the standard deviation as compared with I_A.

Figure 4 shows examples of the linear regression analysis for Tank #1. The results of the stress demand in the tank wall for each IM are presented by using the data set of small amplitude and long distance records (Bin #1). It is evident that the superiority of $S_a(T_1)$ in terms of the efficiency.

The figures also reveal that the long distance ground motion records produce the IMs with higher efficiency. On the other hand, with respect to amplitude, the small amplitude records demonstrate the higher performance of the IMs.

Table 9. Bin #4, large amplitude, long distance

Tank	#1		#2		#3		#4		#5		#6	
	$\beta_{d\|IM}$	R_2	$\beta_{d\|IM}$	R_2	$\beta_{d\|IM}$	R_2	$\beta_{d\|IM}$	R_2	$\beta_{d\|IM}$	R_2	$\beta_{d\|IM}$	R_2
PGA	0.31	0.57	0.32	0.57	0.30	0.61	0.31	0.58	0.60	0.61	0.56	0.69
PGV	0.41	0.21	0.42	0.24	0.41	0.28	0.41	0.25	0.84	0.23	0.77	0.40
PGD	0.43	0.13	0.45	0.14	0.45	0.13	0.45	0.11	0.89	0.12	0.88	0.23
$S_a(T_1)$	**0.13**	**0.92**	**0.13**	**0.92**	**0.12**	**0.94**	**0.11**	**0.94**	0.44	0.78	**0.40**	**0.84**
*S**	0.26	0.69	0.23	0.78	0.22	0.79	0.23	0.78	0.54	0.68	0.52	0.73
I_{NP}	0.17	0.86	0.16	0.89	0.14	0.91	0.15	0.90	**0.43**	**0.80**	0.43	0.81
I_A	0.30	0.57	0.32	0.56	0.32	0.57	0.32	0.55	0.59	0.62	0.61	0.63
CAV	0.33	0.50	0.35	0.48	0.35	0.48	0.35	0.47	0.65	0.53	0.70	0.51
CAD	0.41	0.22	0.42	0.24	0.42	0.24	0.42	0.21	0.83	0.24	0.79	0.37

4.2 IM sufficiency

The sufficiency of the IMs is evaluated by the slope c_1 of the regression line (Eq. 4). The statistical significance of c_1 on M_W or R_{jb} can be quantified by the *p*-value for the F statistic of the null hypotheses ($c_1 = 0$). A small *p*-value, i.e., less than 0.05, suggests that the estimated coefficient c_1 on M_W or R_{jb} is statistically significant, and therefore that IM is insufficient [2].

Results of the comparative statistical analysis relative to IM sufficiency are presented in Table 10 for the 120 records. The values highlighted in bold are associated to *p*-values less than 0.05. In addition, examples of the regression analysis for some representative cases of IMs with regard to Tank #1 are shown in Fig. 5.

The analysis results illustrate no significant correlation between the frequency-dependent IMs and the ground motion parameters, i.e., M_W or R_{jb}, in most of the cases. This demonstrates the sufficiency of this group.

Among the magnitude-dependent group, *PGD* shows a significant degree of insufficiency with respect to both the moment magnitude and the source-to-site distance. On the contrary, *PGA* and *PGV* display their sufficiency for all the analyzed tanks.

Also of note is that the duration-dependent group shows a considerable degree of insufficiency, especially in terms of R_{jb}.

Table 10. Analysis results of the IM sufficiency

Tank	#1		#2		#3		#4		#5		#6	
	p-val (M_W)	*p-val* (R_{jb})	*p-val* (M_W)	*p-val* (R_{jb})	*p-val* (M_W)	*p-val* (R_{jb})	*p-val* (M_W)	*p-val* (R_{jb})	*p-val* (M_W)	*p-val* (R_{jb})	*p-val* (M_W)	*p-val* (R_{jb})
PGA	0.823	0.638	0.574	0.616	0.405	0.607	0.371	0.634	0.857	0.243	0.274	0.659
PGV	0.374	0.258	0.490	0.273	0.525	0.076	0.567	0.083	0.290	0.645	0.117	0.340
PGD	**0.027**	**0.006**	**0.040**	**0.007**	**0.043**	**0.001**	**0.046**	**0.001**	**0.029**	**0.046**	**0.006**	**0.010**
$S_a(T_1)$	0.437	0.823	0.512	0.507	0.159	0.058	0.174	0.063	0.338	0.455	0.156	0.253
*S**	0.778	0.890	0.542	0.746	0.114	0.307	0.114	0.343	0.841	0.328	0.254	0.823
I_{NP}	0.623	0.930	0.356	0.630	0.051	0.110	**0.036**	0.139	0.742	0.368	0.425	0.636
I_A	0.071	0.358	**0.046**	0.398	**0.047**	0.082	**0.033**	0.088	0.283	0.919	0.560	0.500
CAV	0.115	0.061	0.089	0.075	0.095	**0.011**	0.072	**0.012**	0.328	0.444	0.601	0.108
CAD	0.339	**0.021**	0.435	**0.024**	0.435	**0.004**	0.458	**0.005**	0.280	0.127	0.129	**0.036**

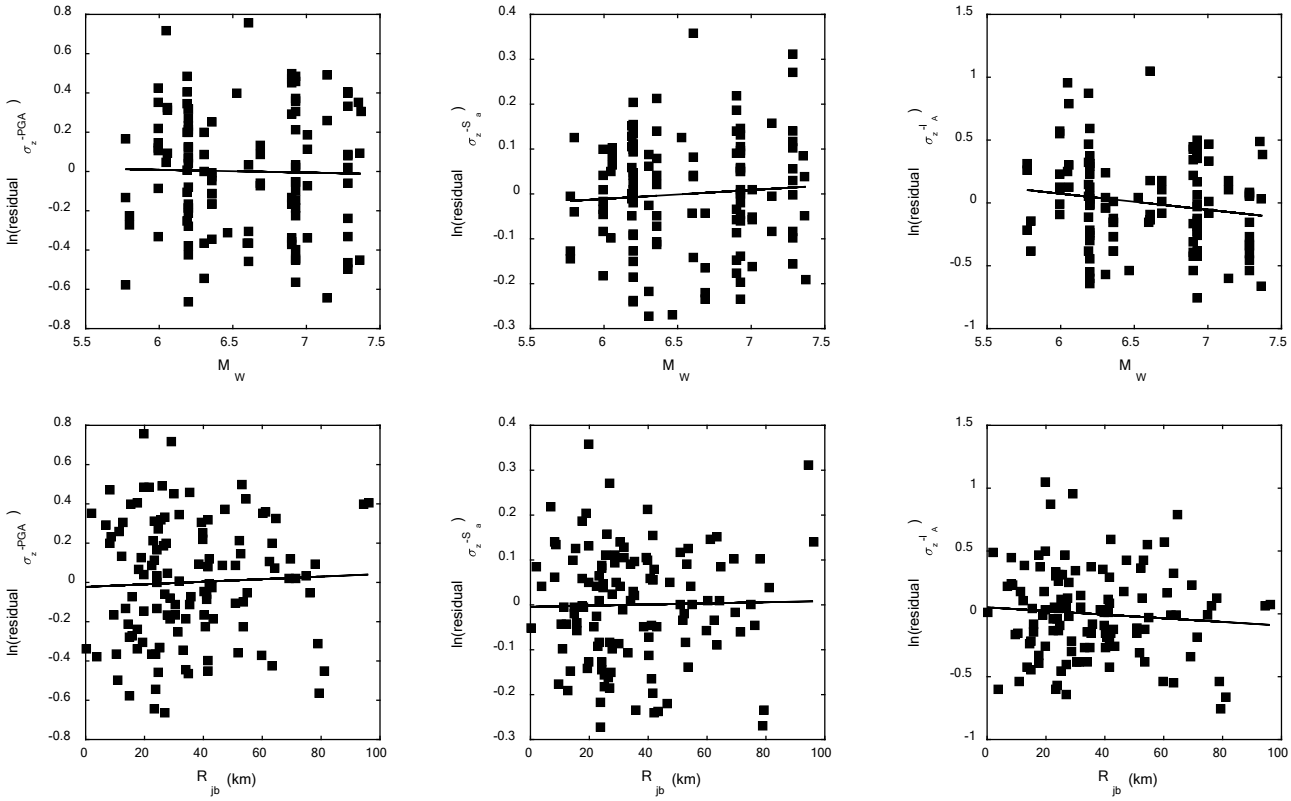

Fig. 5 – Linear regression analysis results of the IM sufficiency for Tank #1

5. Conclusions

In the present paper, a comparative analysis concerning the efficiency and sufficiency of several IMs for the probabilistic seismic demand analysis of steel storage tanks is carried out. A set of magnitude-dependent (*PGA*, *PDV*, *PGD*), frequency-dependent ($S_a(T_1)$, S^*, I_{NP}) and duration-dependent (I_A, *CAV*, *CAD*) IMs are investigated. To evaluate the efficiency of the selected IMs, a linear regression model between EDPs and IMs is used. In particular, the estimate of the median demand is predicted by using a power model. The sufficiency of each IM is also investigated based on a linear regression, which is performed between the residuals of EDPs-IMs and ground motion parameters.

Six cases of tanks, which vary from slender to broad configurations, are analyzed using four sets of ground motion records, representatives of short and long distance natural accelerograms recorded from medium-to-high magnitude seismic events. For this purpose, lumped mass models are used to simulate the seismic behavior of the storage tanks. A comprehensive comparative analysis leads to the following main conclusions:

- $S_a(T_1)$ is the most efficient IM with respect to the meridional stress demand. In addition, the use of I_{NP} leads to similar values of the dispersion with $S_a(T_1)$ while S^* exhibits a significantly lower performance.
- Among magnitude-dependent IMs, *PGA* shows the best performance. In contrast, *PGD* shows the weakest performance, especially in the cases of large amplitude records.
- For duration-dependent IMs, while I_A provides the higher efficiency, *CAV* produces an increase of the standard deviation compared with I_A.
- The long distance ground motion records produce the IMs with more efficiency. In contrast, with respect to amplitude, small amplitude records demonstrate the higher performance of the IMs.
- Regarding to the IM sufficiency, the frequency-dependent IMs also show the sufficiency in terms of M_W and R_{jb}.
- Among the magnitude-dependent group, *PGD* shows a significantly degree of insufficiency. On the other hand, *PGA* and *PGV* display their sufficiency for all the analyzed tanks.

- The duration-dependent group shows a considerable degree of insufficiency, especially in terms of R_{jb}.

6. Acknowledgements

This work has been partially funded by the Italian RELUIS consortium within the executive research program DPC/ReLUIS 2015 and the European Research Project INDUSE-2- SAFETY (Grant No. RFS-PR13056).

7. References

[1] HAZUS (2001): Earthquake loss estimation methodology. National Institute of Building Science, Risk Management Solution, Menlo Park, CA, USA.

[2] Luco N and Cornell CA (2007): Structure-specific scalar intensity measures for near-source and ordinary earthquake ground motions. *Earthquake Spectra*, **23** (2), 357-392.

[3] Shome N, Cornell CA, Bazzurro P and Carballo JE (1998): Earthquakes, records, and nonlinear responses. *Earthquake Spectra*, **14** (3), 469-500.

[4] Shome N and Cornell CA (1999): Probabilistic seismic demand analysis of nonlinear structures. *Reliability of Marine Structures Program Report No. RMS-35*, Dept. of Civil and Environmental Engineering, Stanford University, California.

[5] Luco N (2002): Probabilistic seismic demand analysis, SMRF connection fractures, and near-source effects. *Ph.D. thesis*, Dept. of Civil and Environmental Engineering, Stanford University, California.

[6] Buratti N and Tavano M (2014): Dynamic buckling and seismic fragility of anchored steel tanks by the added mass method. *Earthquake Engineering & Structural Dynamics*, **43**, 1-21.

[7] Phan HN and Paolacci F (2016): Efficient intensity measures for probabilistic seismic response analysis of anchored above-ground liquid steel storage tanks. *In Proceedings of ASME 2016 Pressure Vessels and Piping Conference*, Vancouver, British Columbia, Canada.

[8] Cordova PP, Deierlein GG, Mehanny SSF and Cornell CA (2001): Development of a two-parameter seismic intensity measure and probabilistic assessment procedure. *2nd U.S.-Japan Workshop on PBEE Methodology for Reinforced Concrete Building Structures*.

[9] Bojorquez E and Iervolino I (2011): Spectral shape proxies and nonlinear structural response. *Soil Dynamics and Earthquake Engineering*, **31**, 996-1008.

[10] Arias A (1970): A measure of earthquake intensity. *Final chapter in collection: Seismic Design for Nuclear Power Plants*, MIT Press, Cambridge, MA, 438-469.

[11] EPRI (1988): A Criterion for Determining Exceedance of the Operating Basis Earthquake. *EPRI NP-5930*, Palo Alto, CA.

[12] Cornell C, Jalayer F, Hamburger R and Foutch D (2002): Probabilistic Basis for 2000 SAC Federal Emergency Management Agency Steel Moment Frame Guidelines. *J. Struct. Eng.*, 10.1061/(ASCE)0733-9445(2002)128:4(526), 526-533.

[13] Housner GW (1963): The dynamic behaviour of water tanks. *Bulletin of the Seismological Society of America*, **53**, 381-387.

[14] Haroun MA and Housner GW (1981): Earthquake response of deformable liquid storage tanks. *Journal of Applied Mechanics*, **48**, 411-418.

[15] Veletsos A and Tang Y (1987): Rocking Response of Liquid Storage Tanks. *J. Eng. Mech.*, 10.1061/(ASCE)0733-9399(1987)113:11(1774), 1774-1792.

[16] De Angelis M, Giannini R and Paolacci F (2010): Experimental investigation on the seismic response of a steel liquid storage tank equipped with floating roof by shaking table tests. *Earthquake Engineering & Structural Dynamics*, **39**, 377–396.

[17] Malhotra PK, Wenk T and Wieland M (2000): Simple procedure for seismic analysis of liquid storage tanks. *Structural Engineering International*, 3/2000.

[18] Malhotra PK and Veletsos AS (1994): Uplifting response of unanchored liquid-storage tanks. *J. of Structural Engineering*, **120** (12), 3524-3546.

[19] Phan HN, Paolacci F and Alessandri S (2016): Fragility analysis methods for steel storage tanks in seismic prone areas. *In Proceedings of ASME 2016 Pressure Vessels and Piping Conference*, Vancouver, British Columbia, Canada.

[20] Malhotra PK and Veletsos AS (1994): Beam Model for Base-Uplifting Analysis of Cylindrical Tanks. *J. of Structural Engineering*, **120** (12), 3471-3488.

[21] EN 1998-4 (2006): Eurocode 8: Design of Structures for Earthquake Resistance—Part 4: Silos, Tanks and Pipeline. Brussels, Belgium.